CHAPTER 4

X-RAY NOVA OPHIUCHI 1993 (=GRS 1716-249, V2293 Oph)

And if it takes a couple of years
To turn your tears to laughter...
(McCartney 1984)

4.1. INTRODUCTION

GRS 1716-249 (=X-Ray Nova Ophiuchi 1993) was first discovered as a strong X-ray transient on September 25, 1993 (Ballet et al. 1993); Harmon et al. (1993a) reported that the X-ray spectrum of the object in outburst could be modeled with a power law with spectral index α = 2.0 in the 20÷100 keV band and that, on a broader range of energies, the X-ray spectrum could be better approximated with a thermal bemsstrahlung emission with energy kT = 70 - 100 keV. Differing from that of most SXTs, the X-ray emission from this object was dominated by the hard component (Sunyaev et al. 1994). Only two other X-ray Novae so far showed a similar behaviour: V404 Cyg (Kitamoto et al. 1989, Sunyaev et al. 1991) and, more recently, V518 Per (Sunyaev et al. 1993).

The optical counterpart, V2293 Oph (Fig. 4.1), was discovered at La Silla (Chile) on October 5, 1993 by Della Valle et al. (1994) as a star of magnitude V = 16.65, quite reddened (B-V = 0.9); from a comparison with archival plates, these authors estimated an amplitude of at least 4.4 magnitudes for the optical outburst. The emission lines of H_α (EW = 13.4), H_β (EW = 1.3), and He II λ4686 (EW $\leq$ 1.5), and the interstellar absorption lines at 5780 Å, at 6280 Å and the Na I doublet at 5890 Å (EW = 1.9) were detected in the optical spectra. From the latter value, and from photometric considerations applicable to this kind of objects, these authors computed

an $E(B\text{-}V) = 0.9 \pm 0.2$, and with this value they estimate and upper limit and a mean value for the distance to this system of ≈2.8 kpc and ≈2.4 kpc, respectively.

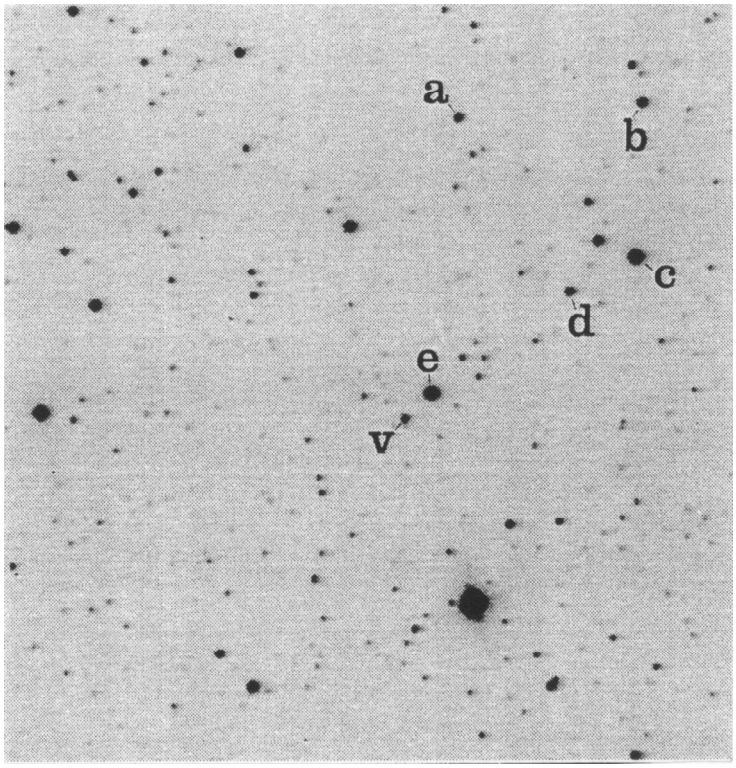

Fig. 4.1. The field of V2293 Oph (=GRS 1716-249) acquired in the *V* filter on October 11, 1993. The exposure time was 2 minutes and the field size is 3′ × 3′. North is at top, East is to the right. Magnitudes of the comparison stars are reported in Table 4.II; the nova is labelled with the 'v' letter.

These authors also reported that the object showed a transient radio emission around the outburst maximum and in the initial stages of the decay: this is a characteristic feature of SXTs (see Sect. 3.4). Using these observations, high-precision coordinates to the system were evaluated: $\alpha = 17^h\ 16^m\ 32^s.52$; $\delta = -24°\ 58'\ 1''.1$ (equinox: 1950).

The X-ray light curve of the X-ray Nova (Fig. 4.2) had a rather long decay time (≈300 days, according to Harmon et al. 1993b) and at least two secondary maxima were observed 11 (Churazov et al. 1994, Borozdin & Alexandrovich 1994, Harmon et al. 1994) and 16 months (Borozdin et al. 1995) after the main one.

In correspondence of the latter X-ray maximum, Karistkaya & Goranskij (1995) observed an optical brightening of the object (their measurements were $V = 17.6$ on April 24, 1995, $V = 17.7$ on April 30, 1995 and $V = 17.2$ on May 10, 1995), thus

indicating the presence of a late minioutburst similar to those seen in other SXTs (see Sect. 4.3 of this Thesis).

Furthermore, van der Hooft et al. (1994) reported the presence of low-frequency QPOs in the X-ray light curve between September 25 and December 14, 1993; the centroid of these QPOs shifted from ~40 mHz a ~80 mHz during the first week of observations and then slowly reached ~300 mHz.

Finally, Hjellming et al. (1996) found the presence of a correlation between X-ray and radio flares occurred in 1995. These authors could not observe any jet or similar structures due to the faintness of the source in the radio band.

In this Chapter the observations of V2293 Oph, mainly performed during the early decline stage, will be reported and analyzed. These observations, as one will see, show the presence of a noisy but real main periodicity (probably a superhump) and of two possibly transient secondary modulations. Using the main periodicity, an estimate of the compact object mass will be given; from this estimate, and from other observational parameters, one will get a strong indication for the presence of a BH harbored in this system.

4.2. OBSERVATIONS AND DATA ANALYSIS

The data, which were all gathered with the ESO telescopes at La Silla (Chile) starting from October 1993, can be divided into two sets: the first one, made by 225 CCD images (168 in the *V*, 56 in the *B* and just 1 in the *R* band), obtained with the 0.92-meter Dutch telescope, deals with the photometric study of the object immediately after the maximum and spans from October 6 to October 15, 1993; the second one instead includes 3 spectra (2 acquired with grism *B300* and 1 with grism #2) and 5 images (1 *B*, 2 *V* and 2 *R*) secured on July 7, 1994 with the 3.6-meter ESO telescope plus EFOSC1 spectrophotometer and on the period February 28 - March 3, 1995 with 3.58-meter ESO NTT telescope plus EMMI spectrophotometer. The complete journal of the observations is reported in Table 4.I.

The frames were corrected for bias and flat field and reduced using the *DAOPHOT II* package (Stetson 1987) and the *ALLSTAR* procedure inside *MIDAS* with a Point Spread Function (PSF) fitting algorithm. To perform relative photometric measurements, 5 comparison field stars (see Fig. 4.1) were chosen on the basis of their *B-V* color, which had to be as much as possible close to that of the X-ray Nova. This choice was made to minimize instrumental effects due to the CCD response.

Table 4.I. Journal of photometric (upper part) and spectroscopic (lower part) observations of V2293 Oph presented in this Chapter.

Date	Telescope	Filter or Passband	Number of Frames	Exposure times (in minutes)
IMAGING				
October 6, 1993	Dutch	*B; V*	1; 3	4; 2
October 7, 1993	Dutch	*B; V*	3; 3	4; 2
October 8, 1993	Dutch	*B; V; R*	9; 29; 1	4; 2
October 9, 1993	Dutch	*B; V*	4; 20	4; 2
October 10, 1993	Dutch	*B; V*	6; 15	4; 2
October 11, 1993	Dutch	*B; V*	6; 19	4; 2
October 12, 1993	Dutch	*B; V*	3; 29	4; 2
October 13, 1993	Dutch	*B; V*	8; 21	4; 2
October 14, 1993	Dutch	*B; V*	5; 20	4; 2
October 15, 1993	Dutch	*B; V*	11; 10	4; 2
July 7, 1994	3.6 m.	*B; V*	1; 1	1
February 28, 1995	NTT	*V; R*	1; 1	0.5
March 3, 1995	NTT	*R*	1	1
SPECTRA				
July 7, 1994	3.6 m.	Grism *B300*	2	30; 45
March 3, 1995	NTT	Grism *#2*	1	15

It was noticed that the internal magnitude differences among the comparison stars were never found to vary more than 0.1 mag from night to night, and more than 0.05 mag during the same night in *B* and *V* photometric bands. Thus, for each frame the difference between the magnitude of the nova and the mean magnitude of the comparison stars was calculated. This reduced the standard deviation for the frames of each single night to 0.01 mag. For this reason, magnitude differences were used in the periodicity analysis.

The magnitudes of the comparison field stars were then calibrated using the stars of the standard Landolt T Phe sequence (Landolt 1992): this allowed the calibration of the *B*, *V*, and *R* magnitudes of the X-ray Nova. Table 4.II reports the magnitudes of the 5 field stars used for this task and shown in Fig. 4.1.

Table 4.II. Johnson *B*, *V* and *R* magnitudes of the comparison stars chosen in the field of V2293 Oph. Magnitude errors are ±0.03 mag for *B* and *V*, and ±0.1 mag for *R*.

Star	*B*	*V*	*R*
a	18.13	16.28	15.0
b	17.64	15.76	14.6
c	15.64	13.86	12.7
d	17.15	15.96	15.2
e	15.23	13.90	13.0

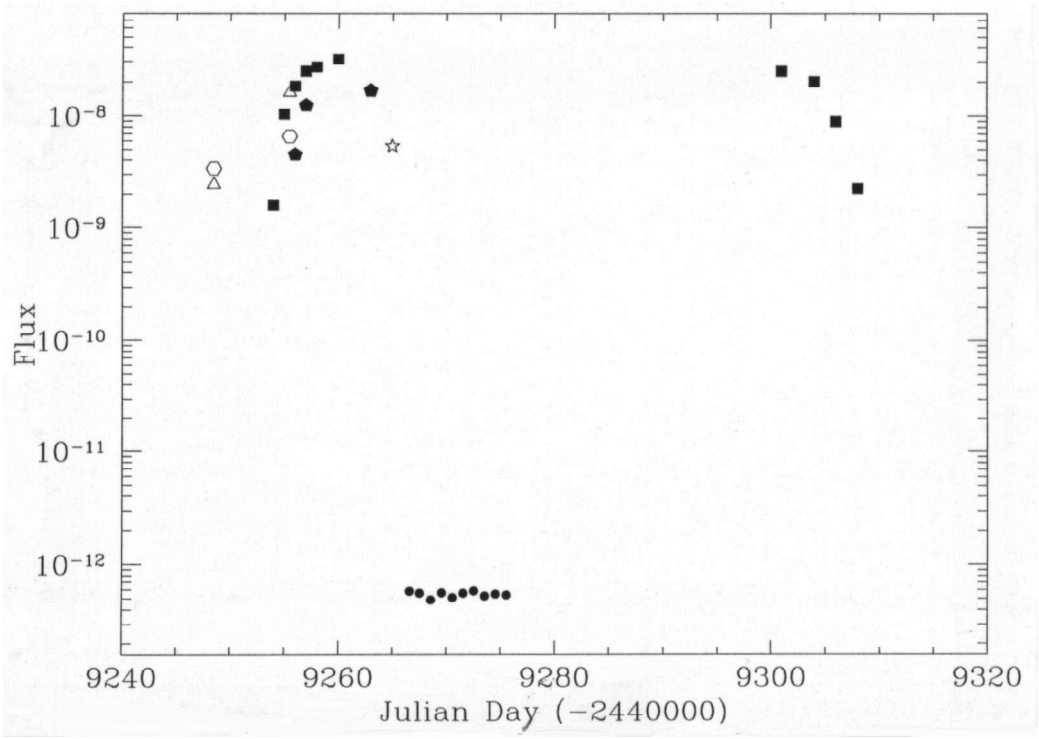

Fig. 4.2. The observed X-ray and *B* light curves of the X-ray Nova. Fluxes are in units of erg cm^{-2} s^{-1}. Symbols indicate different energy bands: 0.5÷10 keV (stars), 12÷17 keV (filled pentangles), 20÷100 keV (filled squares), 35÷150 keV (open triangles), 150÷300 keV (open hexagons) and the October 1993 nightly averaged *B* data reported in this Chapter (filled dots). References for the X-ray data are, in the chronological order, Ballet et al. 1993, Harmon et al. 1993a, Tanaka 1993, Borozdin et al. 1993, Harmon et al. 1993b, and Harmon & Paciesas 1993.

Finally, times at mid-exposure of every imaging frame has been expressed in Heliocentric Julian Days (HJDs) in order to simplify the study of the data time series and mostly to eliminate the effects induced by the motion of the Earth around the Sun.

The spectra were instead reduced using the *IRAF* package. The wavelength calibration was provided using exposures of He-Ar lamp, while flux calibration was performed by means of the spectroscopic standards Feige 110 and LTT 4364. Dereddening for interstellar absorption has been performed using the prescription of Cardelli et al. (1989) and assuming a color excess $E(B\text{-}V) = 0.9$ from Della Valle et al. (1994).

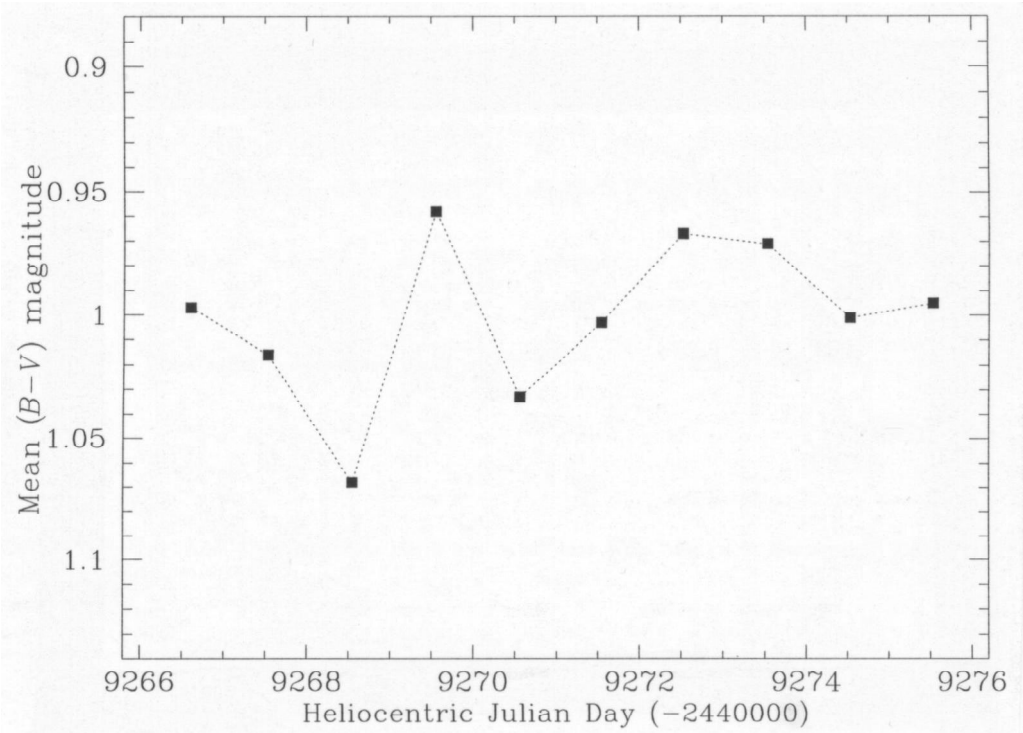

Fig. 4.3. Night-to-night average *B-V* color index variations. The average value over the whole October 1993 observing run yields 1.01 ± 0.02 mag.

Figure 4.2 shows the X-ray light curve of the X-ray Nova and the nightly average fluxes in the *B* band. In Fig. 4.3 the night-to-night modulation of the *B-V* color are instead shown. The variations observed in these average optical light curves are comparable to those found during every night (about 0.2 mag). Single night observations showed light variations as large as those displayed by the average light curve, therefore suggesting activity on time scales of the order of a few hours.

The Discrete Fourier Transform (DFT) and the analysis performed with the *CLEAN* algorithm (Roberts et al. 1987) of the October 1993 *V*-band data (168 points) are shown in Fig. 4.4a,b. The most prominent peak of the DFT amongst the 1-day sampling aliases falls at a period of 2.578 days (hereafter P_1). The power spectrum

shows also the presence of two additional families of aliases, with lower amplitude and centered at higher frequencies (see below). The power spectrum of the October 1993 *B*-band data set (56 points only) presents the same aliases as that of the *V* light curve, but now the strongest peak corresponds to a period of 0.415 days (hereafter P_5). Because of the limited number of data points, an analysis of the whole set of *V* and *B* data points was also tried, after rescaling the average of the *B* magnitudes to the mean *V* value. Obviously, the resulting power spectrum (*B*+*V* data) displays characteristics which are intermediate to the two different sets of data, the more prominent alias now corresponding to 0.719 days (hereafter P_3). However, as a first step, the attention will be focused on the larger and more homogeneous set of *V* data.

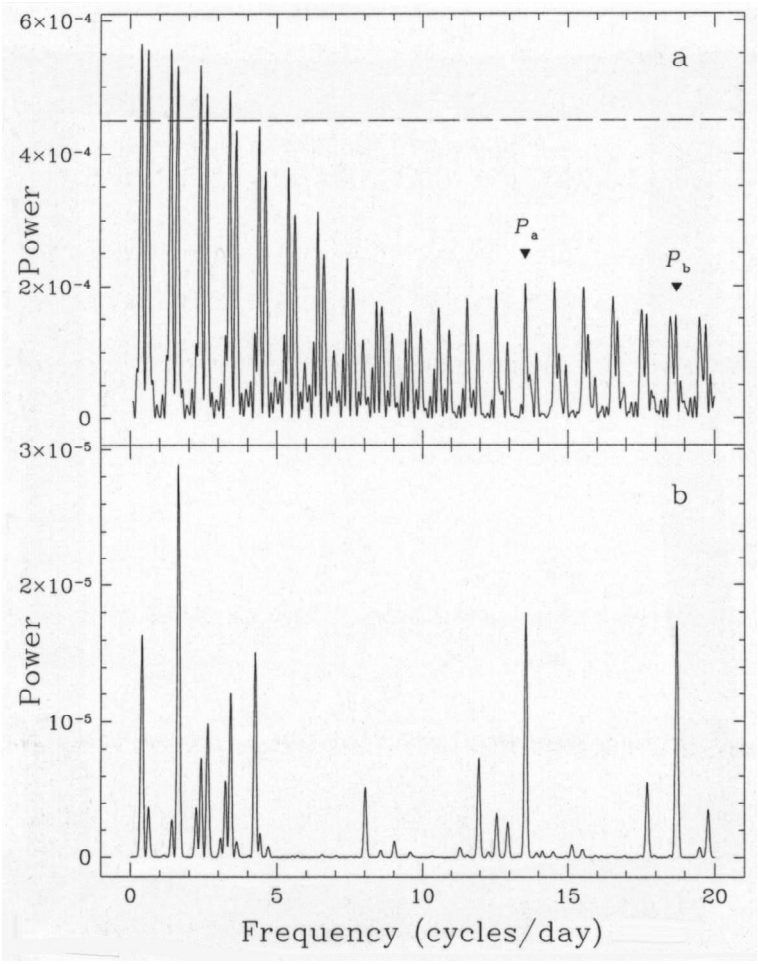

Fig. 4.4. a Raw power spectrum (DFT) of *V* data. The first seven strongest peaks (above the horizontal dashed line) correspond to the periods discussed in the text. 'Odd' and 'even' sequences of peaks represent two specular families of aliases, actually produced by one single signal. **b** *CLEAN*ed power spectrum of *V* data, which displays the P_4 = 0.612689, P_a = 0.07375 and P_b = 0.053416 days modulations as the strongest peaks. P_4 is favoured also by several least-squares methods (see text).

In absence of more precise indications, one might tentatively choose to discuss all the peaks of Fig. 4.4a the power of which is, say, larger than $4.5 \cdot 10^{-4}$. Seven periods, hereafter labelled, with increasing frequencies, P_1, P_2, P_3, P_4, P_5, P_6 and P_7, respectively, are then selected in this way. Note that the odd sequence (P_1, P_3, etc.) and the even sequence (P_2, P_4, etc.) represent two specular families of aliases, both being produced by one single signal, given the structure of the DFT in Fig. 4.4a.

Since the main selected periods range from 7 hours to 2.5 days, it is evident that the nine two-hours observational runs of October 1993 represent, for each periodicity, a rather poor phase-coverage of the light modulation, so that strong sampling effects are introduced. Moreover, the uneliminable effect (the so-called *red noise*; e.g. Vio et al. 1992 and references therein) induced by the flickering, that is, stochastic light variations typical of these systems, will produce an increase of the power at lower frequencies. The situation could result even more entangled in the case of non-sinusoidal signals and in presence of more independent periodicities, as it appears to be in the present case. Thus, the true period of the signal might not be easily detected by means of a simple Fourier analysis.

The *CLEAN*ed power spectrum of V data (Fig. 4.4b) indicates as more probable the peak at 0.612689 days (i.e. P_4) and confirms the presence of two lower amplitude modulations at 0.07375 and 0.053416 days (hereafter P_a and P_b, respectively). These two smaller oscillations of the light curve seem to be independent from each other and also from the main longer period aliases mentioned before. Indeed, each one of these three modulations remains practically unchanged whenever the other two are subtracted.

The *CLEAN*ed power spectrum of the $B+V$ data, instead, favours P_1 (or, possibly, its 1-day alias P_3), but fails to detect the two fainter signals P_a and P_b, although they appear in the raw spectrum and can also be noted in the light curves folded with these periodicity values. One must however remind that the use of the $B+V$ set of data appears somewhat arbitrary because the profile of the signal might be different in different bands (the folded B and V light curves seem to support this possibility; see Fig. 4.5a,b) and also because the B data are affected by larger errors than the V ones

probably because of variable weather conditions particularly during the first days of the October 1993 run.

ome help in the search for the best period may come from visual inspection of the folded light curves. The result is that period P_4 appears to be less characterized by sampling effects than the other ones. In addition, if one subtracts each one of the seven selected main aliases from the data sets and then performs the DFT analysis again, P_4 is found to be the period that better reduces all the aliases once it is subtracted. The same arguments would also justify the choice of P_a and P_b among their own aliases.

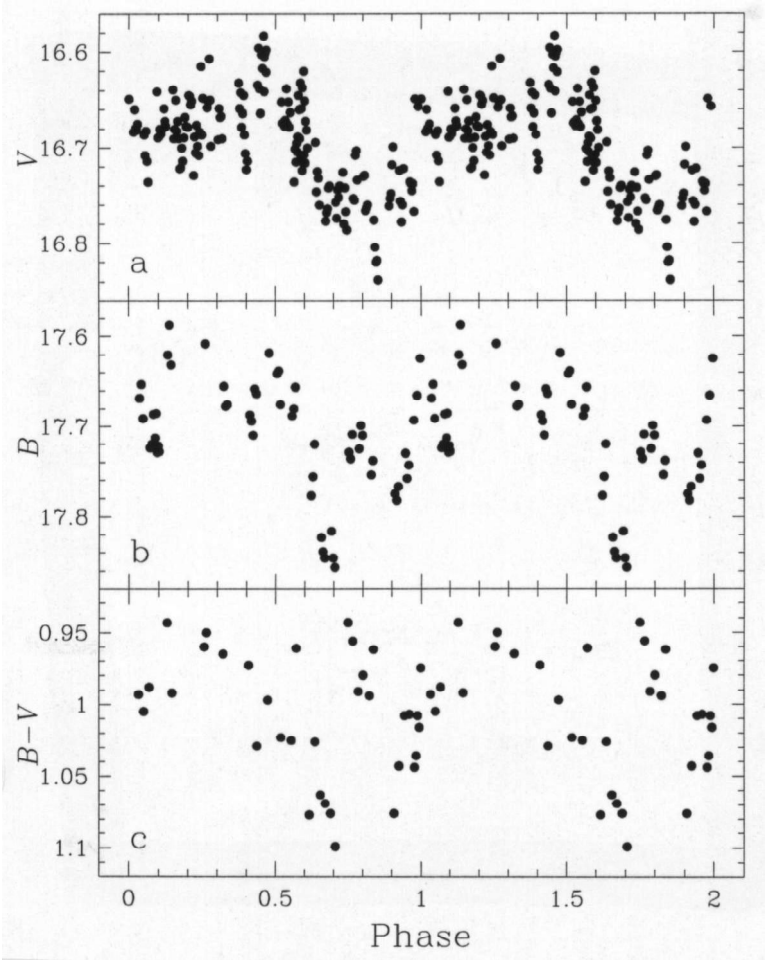

Fig. 4.5a-c. a *V,* **b** *B* and **c** *B-V* folded light curves assuming P_4 as the superhump period; phases are arbitrarily referred to HJD = 0.00. Color index variations are poorly correlated with the superhump cycle, but at light maxima the object appears to be bluer.

As another attempt, numerical experiments by simulating the October 1993 set of data by means of a signal obtained through the superposition of one or more sinusoids have been carried out. The results is that three sinusoids with periods and amplitudes

as those of P_4, P_a and P_b, sampled as the observational data, produced raw and *CLEAN*ed power spectra similar to those of Fig. 4.4a,b, but a better matching was however obtained using P_1 instead of P_4.

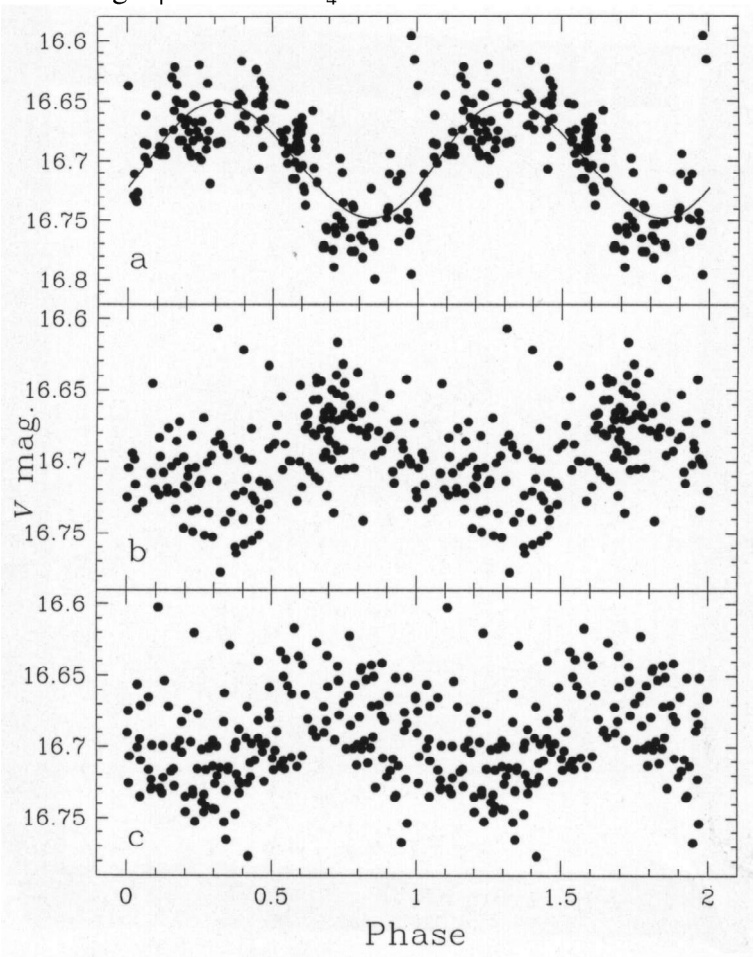

Fig. 4.6a-c. *V* light curves folded with periods **a** P_4, **b** P_a and **c** P_b after subtraction of P_a and P_b, P_4 and P_b, and P_4 and P_a, respectively. Phases are arbitrarily referred to HJD = 0.00. Best fit of data points, i.e. the continuous line in panel (a), suggests an asymmetry which is typical of superhumps and opposite to that of Fig. 4.5a,b. The scattering of the data points in (b) and (c) panels is reduced if only the data of the second half of the October 1993 observing run are used.

So far, these results appear somewhat contradictory; one then needs to look for some other quantitative diagnostics to get further indications. To this aim some methods based on the least-squares algorithm were applied. The results are summarized below:

1) the Renson's method (Renson 1978), by fitting a sinusoid to the data points, finds P_4 as the most probable periodicity of $B+V$ data, but nothing significant is found in the V data;

2) the Barning's method (Barning 1963), which fits a combination of a sinusoid and a cosinusoid to the data points, gives P_4 both using the $B+V$ and the V data sets, although P_2 (=1.597 days) and P_6 (=0.3808 days) cannot be excluded;
3) the Dworetsky's 'string-length' method (Dworetsky 1983) gives no clear results for $B+V$ data, while P_6 is weakly indicated by the V data alone;
4) the Stellingwerf's Phase-Dispersion Minimization (PDM) method (Stellingwerf 1978), which is efficient to use with highly on irregularly spaced data and in presence of a highly non-sinusoidal time variations, suggests P_4 when applied to the V data, but no result is achieved using $B+V$ data.

A brief description of these time-series analysis methods, as well as of the DFT and of the *CLEAN* algorithm, may be found in the Appendix C of this Thesis.

From all this, it can be concluded that, although one is still unable to exclude the other main peaks, most indications are in favour of P_4. The corresponding folded V and B light curves are shown in Fig. 4.5a,b.

The DFT of 35 B-V values, obtained from consecutive B and V determinations, gives no indication and appears as pure noise. Anyway, if one folds these data points with P_4, as shown in Fig. 4.5c, it is found that in coincidence of the light maxima of the above panels only bluer colors are seen for the object.

The single R magnitude determination of October 8, 1993 gives 16.0 ± 0.1 and a V-R color index of 0.7 ± 0.1.

Concerning the shape of folded light curves, most superhump profiles, as already said in Ch. 2, present an asymmetric "sawtooth" shape, i.e. with the rising branch steeper than the decline; actually, the folded light curves of Fig. 4.5a,b seem to show a behaviour which is opposite with respect to that just described. However, the independent nature of the two weaker signals P_a and P_b suggests the opportunity of plotting the V data folded with P_4 after the subtraction of these shorter term periodicities. So, two cosinusoids having amplitudes $A_{a,b} = 2 \cdot \sqrt{\Pi_{a,b}}$ and phases given by the raw Fourier power spectrum, $\Pi_{a,b}$ being the powers of the peaks of the

two signals P_a and P_b, were then subtracted from the V data. The folded light curve of the corrected V data folded with P_4 is shown in Fig. 4.6a. Best fit of the data (see Sect. 4.3.2) would in this case remark a typical slightly asymmetric superhump profile. The same result is found with B magnitudes. The two signals P_a and P_b are represented in Fig. 6b,c, respectively. These two V light curves were obtained in the same way as above by subtracting P_4 and one of the short-term modulations from the data, which were then folded with the remaining short-term perodicity. It was found that in the second half of the October 1993 observing period the amplitudes of P_a and P_b became larger by about a factor two. Therefore, the scattering of the data points of Figs. 4.6b and 4.6c could be reduced if one excludes the observations made in the first days of the October 1993 observations, when the oscillations were barely visible. This might suggest a transient character for the phenomenon. A tendency for a slight decrease of the duration of P_a and P_b, by about 1%, during the second half of the October 1993 run can also be detected.

Let us now consider the photometric observations performed during the decline phase. Those of July 1994 show a clear fading of the object: indeed, it was found at V = 18.90 and B-V = 1.2. A mean B magnitude decay of 0.0089 mag d^{-1} and a mean V magnitude decay of 0.0082 mag d^{-1} with respect to the mean values of October 1993 can be inferred. These decline rates are among the lowest ever found to date for an X-ray Nova; this means that V2293 Oph is one of the slowest X-ray Novae. The February-March 1995 observations showed a brightening of the system up to V = 17.47, with V-R = 0.27 mag. This confirms the existence of a secondary maximum (or minioutburst) observed by Borozdin et al. (1995) in the X-ray band and by Karitskaya & Goranskij (1995) in the optical.

Regarding the spectroscopic observations of the decline, those obtained on July 7, 1994 are characterized by a rather poor signal-to-noise ratio and are not presented because of their low scientific content.

The spectrum of March 3, 1995, taken during the March-April secondary maximum, is instead reported in Fig. 4.7; the optical flux has increased by about one

magnitude with respect to July 1994. The slope of the continuum indicates a rather low temperature, quite far from that estimated by Della Valle et al. (1994) during the early stages of the outburst, but the presence of a faint H_α emission line (EW = 1.42 Å) suggests that accretion onto the compact object was still occurring. No other emission lines are clearly evident. The telluric absorption lines at 6870 Å and 7600 Å, and the interstellar absorption at 5890 Å (NaD doublet; EW = 1.64 Å) are indicated. The interstellar feature at 6280 Å (EW = 2.4 Å) could be significantly contamined by atmospheric absorption, as stated by Callanan et al. (1995).

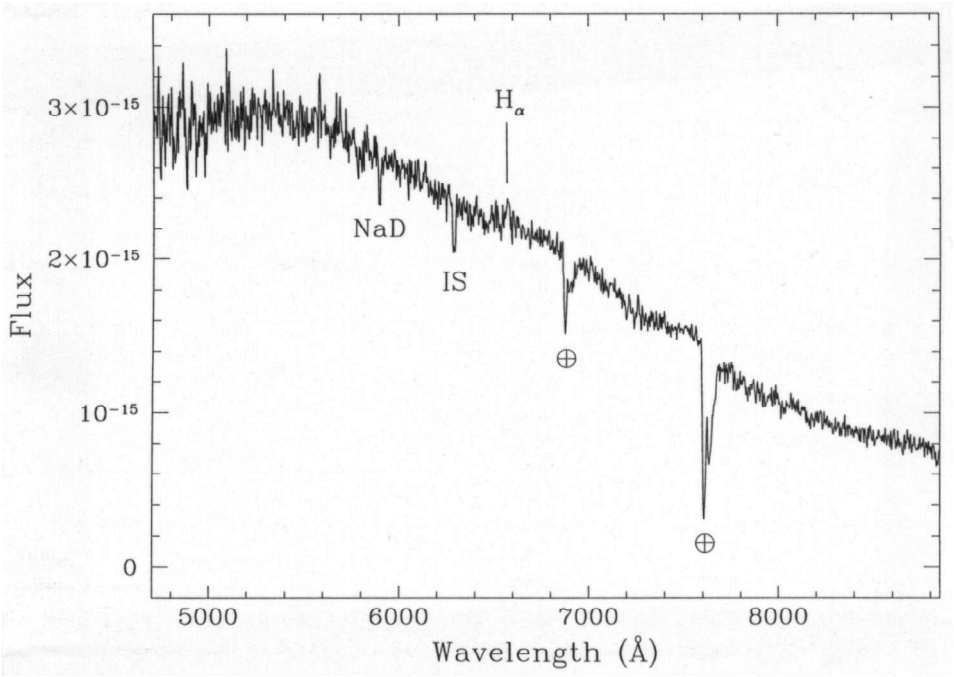

Fig. 4.7. Spectrum obtained on March 3, 1995. It has been dereddened assuming *E(B-V)* = 0.9. Fluxes are in units of erg $cm^{-2}\,s^{-1}$ $Å^{-1}$.

4.3. RESULTS AND DISCUSSION

4.3.1. The mass of the compact object

Since its discovery, V2293 Oph showed an X-ray behaviour typical of SXTs containing a BHC. Indications in favour of a high-mass primary in this system might be given also by the presence of superhumps in the optical light curve.

Superhumps are believed to occur in close binary systems (see Sect. 2.4) when two conditions are met:

1) the mass ratio q of the system is lower than 0.25-0.33, so that a resonant behaviour of the accretion disk in the potential well of the secondary can be triggered (Whitehurst & King 1989, 1991);
2) the accretion disk experiences enhanced mass transfer rates as large as 10^4 - 10^5 times than the typical value at quiescence (Vogt 1982).

Della Valle et al. (1994) derived for the distance to V2293 Oph an upper limit of ≈2.8 kpc. This implies, using the estimate on the quiescent optical magnitude given by these authors, a luminosity of the system at quiescence typical of a late type main sequence star of spectral type K or later. For this reason, and also by analogy with other SXTs which possess low mass secondaries (see also Martin et al. 1995), one can infer for the secondary a conservative upper limit of ~1 $M_\odot$.

If one supposes that SXTs have Roche-lobe filling secondaries, item [2] should be satisfied, in particular during the outburst of V2293 Oph. Indeed, as pointed out by Bailyn (1992), whether or not mass transfer instabilities occur in outbursting SXTs, an enhancement of the mass transfer rate from the secondary should always be guaranteed by the strong heating of the secondary itself by the X-ray flux from the primary. This would also explain why the outbursts of SXTs last longer and are more variable than DN superoutbursts (Mineshige 1994).

Thus, if what it is observed in V2293 Oph is indeed a superhump phenomenon, and item [1] is also satisfied, the mass of the primary should be higher than 3 $M_\odot$.

A simple formula which gives a lower limit to the mass of the primary of SXTs, given by Mineshige et al. (1992), using the analogy between the outbursts of these systems and the superoutbursts of SU UMa-type DNe and assuming for q the more restrictive upper limit of 0.33, is Eq. (2.7). Using this formula one finds that, if P_{sh} = P_4 (~14.7 hours), the mass of the secondary is 1.6 $M_\odot$, and the lower limit to the mass of the primary is ≈4.9 $M_\odot$. Period P_3 (~17.3 hours), being close to P_4, leads to a similar conclusion, with a secondary of 1.9 $M_\odot$ and a primary of 5.7 $M_\odot$. One can note that in both cases secondaries more massive and more luminous than the Sun are

obtained. These secondaries would then be substantially brighter than what suggested by Della Valle et al. (1994). One possibility is that the determination of the distance of the object has been underestimated. Or, perhaps, the secondary is a slightly evolved late type star.

If one instead assumes $P_{sh} = P_1$ (~2.58 days), an even more massive or an evolved secondary is obtained and one is no longer allowed to use Eq. (2.7). Such a system might however be similar to the X-Ray Nova Scorpii 1994 (=GRO 1655-40), which, according to Bailyn et al. (1995b), has an orbital period of 2.62 days, $M_1 \sim 5.4\ M_\odot$ and $M_2 \leq 1.5\ M_\odot$. This last hypothesis is however unlikely because it would imply a remarkably larger luminosity of V2293 Oph at quiescence, in disagreement with the results by Della Valle et al. (1994). Similar argumentations would lead to avoid the choice of P_2 (~1.59 days).

The assumption of the shorter P_5, P_6 or P_7 (~0.29 days) periods would more easily allow the hypothesis of a Roche-lobe filling low-mass main sequence secondary, in analogy with V616 Mon (McClintock & Remillard 1986) or with GU Mus (Remillard et al. 1992). Thus, in this case, Eq. (2.7) is more likely applicable, giving for M_1 lower limits of 3.3 $M_\odot$, 3.0 $M_\odot$ and 2.3 $M_\odot$ for P_5, P_6 and P_7, respectively. Anyway, one must remember that this analysis tends to favour P_4 above the other periods.

The use of the approach proposed by Mineshige et al. (1992) has however to be taken with some degree of caution because of the issues pointed out in the previous Chapter.

A massive primary may be also suggested by the very long decay time of the X-ray light curve of this X-ray Nova. This rate of decline is indeed, as remarked in Sect. 3.4, a function of the mass of the compact object and of the viscosity of the accretion disk (Mineshige et al. 1993). The observed *e*-fold time, $\tau_{1/e}$, of V2293 Oph is ~300 days (Harmon et al. 1993b), and is by far the largest among known SXTs. Now, by using (3.10) and by adopting the mass estimates for V616 Mon (McClintock & Remillard 1986), V404 Cyg (Shahbaz et al. 1994), QZ Vul (Charles & Casares 1995) and GU Mus (Remillard et al. 1992) together with their *e*-fold times, it is evident that the mass

of the primary of V2293 Oph can be smaller than that of these BHXN only if one assumes that the viscosity inside the accretion disk is much smaller (by a factor 50, at least) than that assumed for the other SXTs.

All this still plays in favour of the existence of a massive compact object inside V2293 Oph.

4.3.2. The superhump light curve

Several models have been proposed to explain the superhump phenomenon (see Warner 1985 and Whitehurst 1988a for a review). The superhump light curve of V2293 Oph is represented in Fig. 4.6a; the independent secondary modulations P_a and P_b have been removed from it. The mean profile is slightly asymmetric with the rise steeper than the decline. Such a "sawtooth" shape seems to be quite a general feature of superhump light curves, but no clear explanation has been given so far.

A promising interpretation of the superhump phenomenon has been given by Whitehurst & King (1989, 1991) in terms of an elliptic disk which is precessing due to the tidal action of the secondary. The light modulation should be produced by periodic variations in the efficiency of dissipative processes in the accretion disk and this would account for the lack of correlation between the amplitude of superhumps and the orbital inclination (Warner 1995). However, as noticed by O'Donoghue (1990), a direct comparison of this theoretical model with the observed light curves is still premature.

So, one can adopt here the simple prescription proposed by Vogt (1982) based on the presence of an elliptic disk plus an hot spot where the potential energy of the stream of matter coming from the secondary is released. The light modulation should be the result of the gas flow impacting the outer edge of the disk at a continuously and cyclically changing distance from the primary. If the stream does not penetrate too deep in the disk, then the impact energy will be mainly redistributed over the outer rim of the disk. This might explain why superhumps rarely undergo eclipses. It is

worth noting that recent results seem to place the superhump source right in the cooler edge of the disk (O'Donoghue 1990).

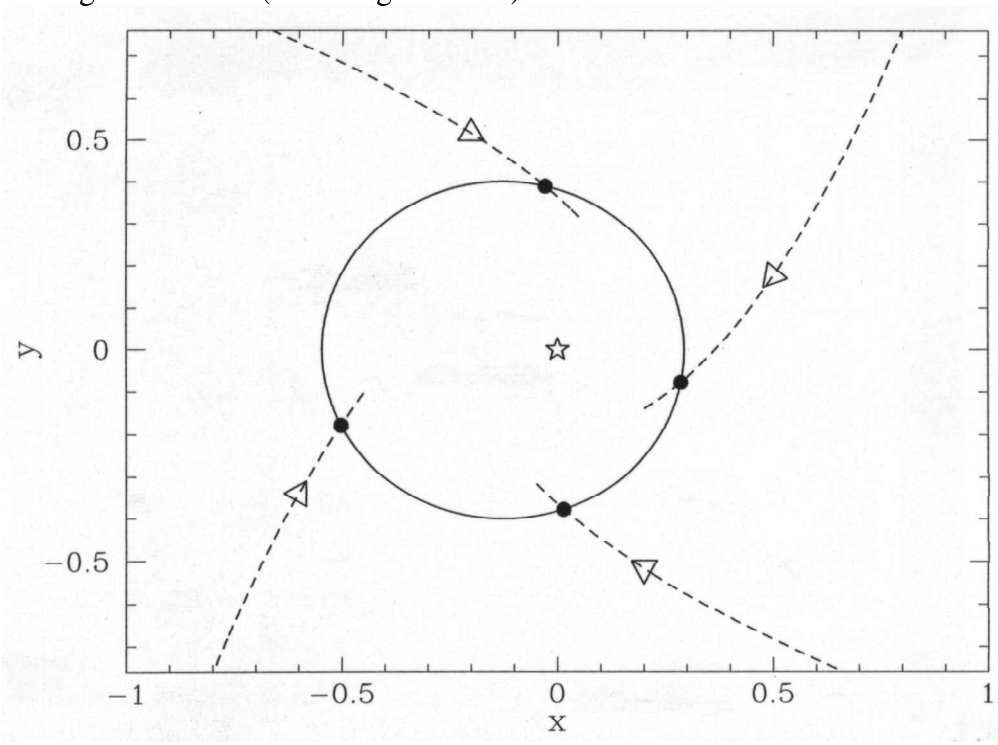

Fig. 4.8. Geometry of the gas stream impacting the elliptic disk in correspondence of four equally spaced orbital phases. Divisions on the axes are in units of the orbital separation a. The star located at the origin of the axes indicates the position of the compact primary.

Using the geometry of the stream described by Lubow & Shu (1976), the impact radius with the precessing elliptic disk can be calculated. A graphic representation of the gas stream impacting an elliptic disk is given in Fig. 4.8. Then, by indicating as β the ratio between the modulated luminosity of the hot spot region and that of the whole disk, one may compute light curves for a variety of input parameters. As an example, Fig. 4.9 shows the light curve for $q = 0.07$, $e = 0.5$, $\beta = 0.2$ and $a_{ell} = 0.42a$, where q is the mass ratio of the system, e is the eccentricity of the disk, and a_{ell} is its semimajor axis in units of the orbital separation, a. Geometric parameters for the disk have been chosen according to the model of superoutbursts of SU UMa-type DNe made by Whitehurst (1988b), and β was determined in order to produce superhumps with a ≈0.2 mag amplitude, typical of the phenomenon.

Assuming for V2293 Oph the same mass ratio, q, used in the geometric example of Fig. 4.9 (the final results are however not strongly dependent on this parameter when it is smaller than 0.5), the best fit of the observed superhump light curve of V2293

Oph with this model yields $\beta = 0.11$ and $e = 0.1$ (see Fig. 4.6a). Such an eccentricity is appreciably smaller than that suggested by Whitehurst (1988b). However this might be the effect of a stream which penetrates deeper in the disk smearing out the light modulation of the hot spot. Anyway, it is possible that a more detailed treatment of Whitehurst's (1988b) model will give an alternative and more quantitative interpretation of the observed slightly asymmetric superhump lightcurves.

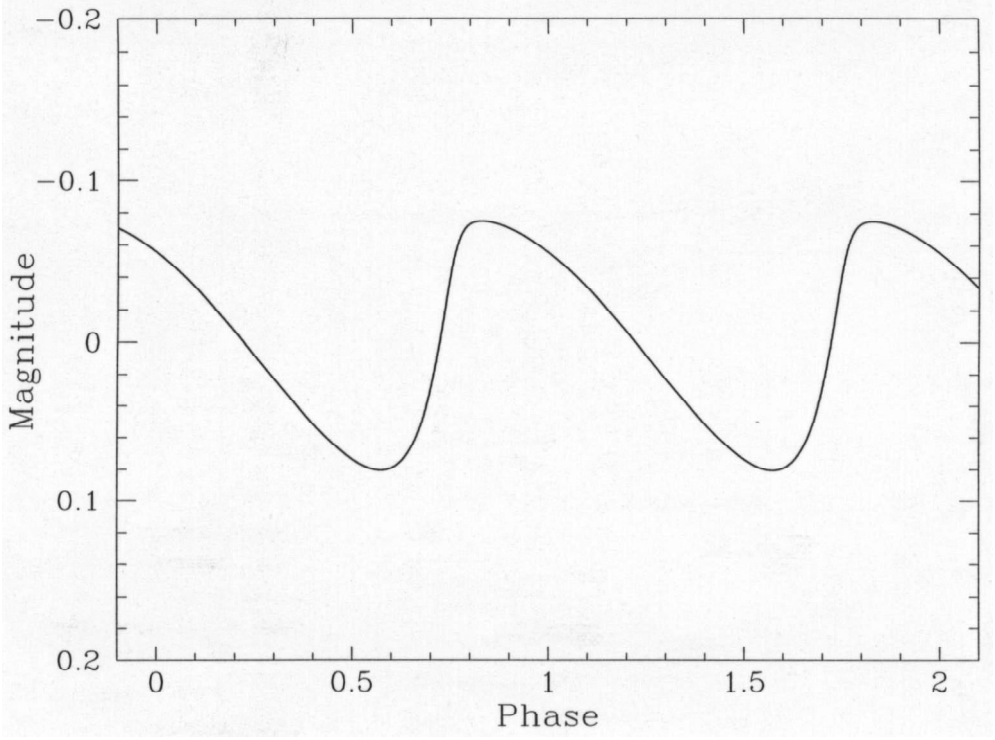

Fig. 4.9. Theoretical light curve produced by the superhump hot spot model (see text), for a mass ratio $q = 0.07$, an eccentricity of the disk $e = 0.5$, a semimajor axis of the disk $a_{ell} = 0.42a$, and $\beta = 0.2$; the latter quantity represents the fractional area of the disk (hot spot or annulus) where the light modulation is produced.

A deeper analysis of the superhump light curve model illustrated and applied here as well as the *FORTRAN* code written for describing it in a quantitative way can be found in the Appendix A of this Thesis.

4.3.3. The color of the system and the short-term modulations

As it was seen before, the observed *B-V* color of V2293 Oph during the early outburst is variable within 0.2 mag and, on the basis of our relatively scanty statistics, color variations seem to be poorly correlated with the superhump cycle.

Strong *V-I* variations have been observed in X-Ray Nova Scorpii 1994 (=GRO J1655-40); these were likely due to eclipses (Bailyn et al. 1995a). On the contrary, if no eclipses are observed no periodic variations of the color indices seem to be present in SXTs. Bailyn (1992), for instance, did not find any modulation of the *B-V* color index in GU Mus during the outburst. The folded *B-V* lightcurve of V2293 Oph (see Fig. 4.5c) however shows that, in spite of a rather flickered behaviour (the presence of rapid flickering might compromise the simultaneity of consecutive *B* and *V* observations), the object appears to be bluer at periodic light maxima. This might suggest the existence of a weak modulation of *B-V* color index with the superhump cycle.

The nature of P_a and P_b is quite puzzling. They do not seem to be correlated with the main period P_4; they probably represent transient phenomena, almost absent at the very beginning of October 1993 observations. It has however to be noticed that shorter secondary oscillations have been observed in MM Vel (=GRS 1009-45, =X-Ray Nova Velorum 1993) by Bailyn and Orosz (1995), and a 6-hour secondary modulation was detected in V404 Cyg also at quiescence (Gotthelf et al. 1992, Casares et al. 1993).

According to Lubow (1989), part of the matter flow from the secondary is not stopped by the collision with the outer edge of the accretion disk and flows over it. Then, the stream falls back onto the disk near the radius of closest approach to the compact object, forming vertical structures ('blobs') which will follow elliptical orbits. All this should approximately occur at about the circularization radius ($\approx 0.2a$ in the case of V2293 Oph) where keplerian velocities are consistent with the observed short-term modulations. Blobs of material orbiting in the disk might also be the consequence of occasional enhancements of the mass transfer rate from the secondary. One can note that the tendency of P_a and P_b to evolve towards larger amplitudes and shorter periodicities is generally expected from such blobs orbiting in the disk. This scenario is also consistent with the trend exhibited by the mean *B-V* to become bluer during the second part of the October 1993 run (see Fig. 4.3).

REFERENCES OF CHAPTER 4

- Bailyn, 1992, ApJ, 391, 298
- Bailyn C.D., Orosz J.A., 1995, ApJ, 440, L73
- Bailyn C.D., Orosz J.A., Girard T.M., 1995a, Nat, 374, 701
- Bailyn C.D., Orosz J.A., McClintock J.E., Remillard R.A., 1995b, Nat, 378, 157
- Ballet J., Denis M., Gilfanov M., Sunyaev R.A., 1993, IAU Circ. 5784
- Barning F.J.M., 1963, BAN, 17 (n. 1), 22

- Borozdin K., Alexandrovich N., 1994, IAU Circ. 6083
- Borozdin K., Arefiev V., Sunyaev R.A., 1993, IAU Circ. 5878
- Borozdin K., Alexandrovich N., Sunyaev R.A., 1995, IAU Circ. 6141
- Callanan P.J., Garcia M.R., McClintock J.E. et al., 1995, ApJ, 441, 786
- Cardelli J.A., Clayton G.C., Mathis J.S., 1989, ApJ, 345, 245
- Casares J., Charles P.A., Naylor T., Pavlenko E.P., 1993, MNRAS, 265, 834
- Casares J., Charles P.A., Marsh T.R., 1995, MNRAS, 277, L45
- Chevalier C., Ilovaisky S.A., 1995, A&A, 297, 103
- Churazov E., Gilfanov M., Ballet J., Jourdain E., 1994, IAU Circ. 6083
- Della Valle M., Jarvis B.J., West R.M., 1991, Nat, 353, 50
- Della Valle M., Mirabel I.F., Rodriguez L.F., 1994, A&A, 290, 803
- Dworetsky M.M., 1983, MNRAS, 203, 917
- Gotthelf E., Halpern J.P., Patterson J., Rich R.M., 1992, AJ, 103, 219
- Harmon B.A., Paciesas W.S., 1993, IAU Circ. 5913
- Harmon B.A., Zhang S.N., Paciesas W.S., Fishman G.J., 1993a, IAU Circ. 5784
- Harmon B.A., Fishman G.J., Paciesas W.S., Zhang S.N., 1993b, IAU Circ. 5900
- Harmon B.A., Zhang S.N., Paciesas W.S., Wilson C.A., Fishman G.J., 1994, IAU Circ. 6104
- Karitskaya E.A., Goranskij V.P., 1995, IAU Circ. 6174
- Kitamoto S., Tsunemi H., Miyamoto S. et al., 1989, Nat, 342, 518
- Landolt A.U., 1992, AJ, 104, 340
- Lubow S.H., 1989, ApJ, 340, 1064
- Lubow S.H., Shu F.H., 1976, ApJ, 207, L53
- Mineshige S., 1994, ApJ, 431, L99
- Mineshige S., Hirose M., Osaki Y., 1992, PASJ, 44, L15
- Mineshige S., Yamasaki T., Ishizaka C., 1993, PASJ, 45, 707
- O'Donoghue D., 1990, MNRAS, 246, 29
- Remillard R.A., Orosz J.A., McClintock J.E., Bailyn, C.D., 1996, ApJ, 459, 226
- Renson P., 1978, A&A, 63, 125
- Roberts D.H., Lehár J., Dreher J.W., 1987, AJ, 93, 968
- Stellingwerf R.F., 1978, ApJ, 224, 953
- Stetson P.B., 1987, PASP, 99, 191
- Sunyaev R.A., Kaniovskij A.S., Efremov V.V. et al., 1991, SvA Lett., 17, 123
- Sunyaev R.A., Kaniovskij A.S., Borozdin K.N. et al., 1993, A&A, 280, L1
- Tanaka Y., 1993, IAU Circ. 5877
- van der Hooft F., Kouveliotou C., van Paradijs J. et al., 1996, ApJ, 458, L75
- Vio R., Cristiani S., Lessi O., Provenzale A., 1992, ApJ, 391, 518
- Vogt N., 1982, ApJ, 252, 653
- Warner B., 1995, Cataclysmic Variable Stars. Cambridge Univ. Press, Cambridge
- Whitehurst R., 1988a, MNRAS, 232, 35
- Whitehurst R., 1988b, MNRAS, 233, 529
- Whitehurst R., King A.J., 1989, Superhumps in accretion discs. In: Hunt J., Battrick B. (eds.) Proc. 23rd ESLAB Symposium on Two Topics in X-Ray Astronomy (ESA SP-296). ESA Publication Division, ESTEC, Noordwijk, vol. 1, p. 127
- Whitehurst R., King A.J., 1991, MNRAS, 249, 25